



UPCommons

Portal del coneixement obert de la UPC

<http://upcommons.upc.edu/e-prints>

Tarrasó, Andrés; Candela, José Ignacio; Rocabert, Joan; Rodríguez, Pedro (2017) Proportional-resonant current controller with orthogonal decoupling on the $\alpha\beta$ -reference frame. *IECON 2017 - 43rd IEEE Annual Conference of the IEEE Industrial Electronics Society, Beijing, China, Oct. 29 – Nov. 1, 2017: proceedings*. [S.l.]: IEEE, 2017. Pp. 1453-1458 Doi: 10.1109/IECON.2017.8216247

© 2017 IEEE. Es permet l'ús personal d'aquest material. S'ha de demanar permís a l'IEEE per a qualsevol altre ús, incloent la reimpressió/reedició amb fins publicitaris o promocionals, la creació de noves obres col·lectives per a la revenda o redistribució en servidors o llistes o la reutilització de parts d'aquest treball amb drets d'autor en altres treballs.

Proportional-Resonant Current Controller with Orthogonal Decoupling on the $\alpha\beta$ -Reference Frame

Andres Tarraso, Jose Ignacio Candela, Joan Rocabert
Technical University of Catalonia (UPC)
Research Center on Renewable Electrical Energy Systems
(SEER Center), Terrassa, SPAIN
andres.tarraso@upc.edu

Pedro Rodriguez
Universidad de Loyola
Sevilla, SPAIN
prodriguez@uloyola.es

Abstract— The increasing penetration of grid-connected RES systems, advanced control algorithms have been developed to operate under grid faults and fulfill strict requirements of the grid codes. In order to overcome this, the current controller performance is critical considering it as the inner control loop of any grid-connected RES system. Based on the resonant control concept, this paper presents a modified structure for this controller which results advantageous when implemented on RES systems, as it permits better performance during the dynamic state of the controller. This paper also deals with the analysis of the decoupling terms in the $\alpha\beta$ reference frame, as well as the capability to generate a decoupled control of the positive and the negative sequence. The proposed controller will be analyzed, discussed and finally validated by means of simulation analysis.

Keywords—*decoupling; current controller; RES; $\alpha\beta$ -reference frame;*

I. INTRODUCTION

In the recent years, the integration of renewable energy systems (RES) to the electrical network has been exponentially increasing, reaching in some countries a 40% of the annual electrical energy demand coverage. However, those systems have a lack of inertia compared to the classical synchronous systems, which means a strong difference on dynamics. The adaptation of all international grid codes is a good example [1] of the penetration of this renewable systems. This evolution on grid codes and control of grid-tied power converters is the base for the huge increase of RES based generation systems connected to the grid. This has forced to devote remarkable efforts to study in which direction the integration of renewable systems should be conducted forcing researchers to dedicate a lot of efforts to study the direction of the integration of renewable systems, to make a proper integration of those system to the electrical network.

Grid codes around the globe are being modified and some are adding specific requirements to harmonize the operation of the electrical system in a safe way with the penetration of renewable energy sources, which have an important impact as the power installed increases [2]. The incoming modifications on the grid requirements are mainly oriented to modify certain operation in the generation systems based on RES, which

influences on its dynamic at the most inner level of the power conversion stages, as most of them count on power electronics converters as an interface to the electrical network. Those increasing restrictions force the power converters to be more stable, faster and able to operate under grid fault offering a determined power profile required by the grid [3].

In order to satisfy the modified requirements of the incoming grid code for RES systems [4], inner control loops should be enhanced [5]. To contribute on solving this issue, an improved control loop able to maintain a good controllability and even improve the dynamic performance through grid perturbations for power converters will be proposed in this paper, where a decouple matrix to avoid active and reactive power coupling is achieved under transient conditions to ensure the good performance of the inverter even under fault conditions. Despite the fact that there are many different linear controllers, PI based controllers working in the dq -stationary reference frame have been by far the most implemented control for grid-connected power converters. In these controllers it is possible to decouple the active and the reactive power via using a cross-coupling term [6]. Another control method is the PR controller [7] applied in the $\alpha\beta$ -reference frame. This second controller does not include such cross-coupling [8].

This paper presents a modified PR current control schematic strategy for the PR controller, which has been selected as the basic current control strategy, due to the fact that its implementation is easier and requires no phase estimation, only frequency, which is a more stable variable if compared with phase angle [5]. In the following sections a comparison between different PR controller structures and their main differences will be performed. Afterwards the modified PR controller will be presented and its capability for controlling separately positive and negative components, also a demonstration of the cross-coupling terms appearing on the $\alpha\beta$ -reference frame to decouple active and reactive power during transients. Simulation results of the different current controllers are going to be done in order to compare them on dynamics and steady state.

II. CURRENT CONTROLLER

The PI and the PR controllers can be assumed as an equivalent controller that work on a different reference frame [9]. For this reason both controllers have a straight relation. It is a matter of a transformation between reference frames to change a PI controller in the dq- frame into a PR controller in the $\alpha\beta$ domain.

A. TRADITIONAL SOGI PR CONTROLLER

The traditional structure of the PR controller is generally known as the second order general integrator (SOGI) [10], that is able to achieve infinite gain at the resonance frequency. This controller structure is presented in Fig. 1.

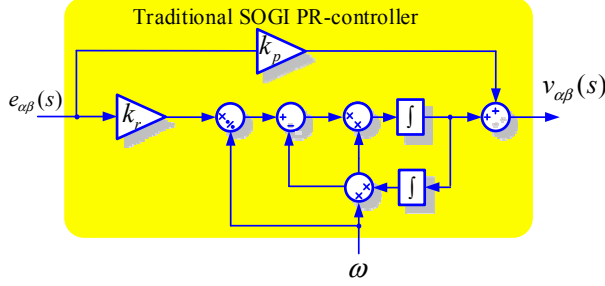


Fig. 1: Traditional SOGI PR controller implementation on the continuous domain

With infinite gain at the resonance frequency the SOGI PR controller is able to offer a good dynamic step performance and zero steady state error [11]. The SOGI PR structure transfer function is the following:

$$G(s) = k_p + \frac{2 \cdot k_r \cdot s}{s^2 + \omega^2} \quad (1)$$

The transfer function of the SOGI PR controller can be achieved also by transforming the traditional PI controller. the PI transfer functions is the one shown in (2), working on the dq-reference frame [7].

$$\mathbf{H}(s)_{PI,dq^+} = \begin{bmatrix} k_p + \frac{k_i}{s} \\ k_p + \frac{k_i}{s} \end{bmatrix} \quad (2)$$

Considering ω as the resonance frequency of the controller, the rotation of the PI results in a PR controller structure and it can be written as shown in (3)

$$\mathbf{H}(s)_{PR,\alpha\beta^+} = \begin{bmatrix} k_p + \frac{k_r s}{s^2 + \omega^2} & \frac{k_r \omega}{s^2 + \omega^2} \\ -\frac{k_r \omega}{s^2 + \omega^2} & k_p + \frac{k_r s}{s^2 + \omega^2} \end{bmatrix} \quad (3)$$

When (2) is rotated, equation (2) and (3) are equivalent, that means that the relation of PI on the dq-reference frame, and a PR on the $\alpha\beta$ -reference frame is mainly the park transformation.

As it is well known, the PI controller is specific for the positive sequence of the system. This means that equation (3) is specifically only for positive sequence. If the addition of the negative sequence into the equation is done the crossed functions change its sign, as shown in (4).

$$\mathbf{H}(s)_{PR,\alpha\beta^-} = \begin{bmatrix} k_p + \frac{k_r s}{s^2 + \omega^2} & -\frac{k_r \omega}{s^2 + \omega^2} \\ \frac{k_r \omega}{s^2 + \omega^2} & k_p + \frac{k_r s}{s^2 + \omega^2} \end{bmatrix} \quad (4)$$

If equation (3) and (4) are directly implemented as the current controller, taking into account that only one proportional gain is needed, the final result ends as (5).

$$\mathbf{H}(s)_{PR,\alpha\beta^-} = \begin{bmatrix} k_p + \frac{2k_r s}{s^2 + \omega^2} & 0 \\ 0 & k_p + \frac{2k_r s}{s^2 + \omega^2} \end{bmatrix} \quad (5)$$

Which matches equation presented on (1). That means that the traditional PR controller has the capability to control both the positive and the negative sequence, using only one equation. This has a strong drawback which is that this PR controller implementation, on the positive and negative control, have the same parameters, affecting the controllability of the whole system.

B. PR BANDWIDTH CONTROLLER

The implementation of equation (1) on the digital domain has some issues, mainly due to the infinite gain at the resonance frequency creating an overflow values on the discrete domain, which makes the controller very fast but also susceptible to produce peaks at the output [12]. For this reason in some applications the controller is forced to have a bandwidth limitation [13], having thus a non-infinite gain trying to limit the actuation of the controller. This additional gain reduces the response at the resonance frequency, but still provide a good performance if it is tuned accurately [14]. The transfer function of the limited PR bandwidth controller is shown in (6).

$$G(s) = k_p + \frac{2k_r \omega_c s}{s^2 + 2\omega_c s + \omega^2} \quad (6)$$

This expression can be achieved by rotating a low pass filter into the $\alpha\beta$ -reference frame, instead of rotating directly a PI. The implementation on the continuous domain of the bandwidth PR controller is presented in Fig. 2.

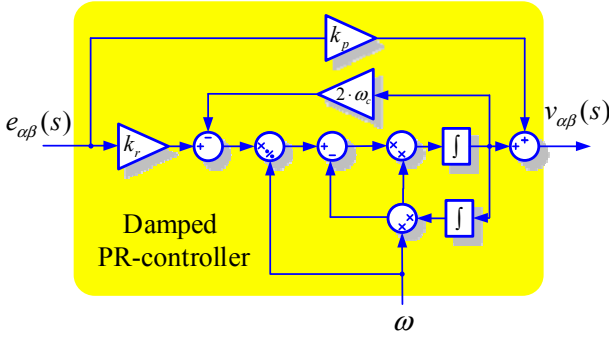


Fig. 2: Bandwidth PR controller implementation on the continuous domain

Those two PR structures, SOGI classical PR controller and bandwidth PR controller, have been highly used in the current control loops of grid-connected inverters. However, with those structures it is not possible to control separately the positive and the negative sequence. In both cases the same control parameters are set to k_r and k_p , which are applied for the positive and the negative components.

Because of this a proposal of a PR that can operate differently for the positive and negative sequence is going to be presented, as well as a decoupling term appearing on dynamic states.

III. PROPOSED PR STRUCTURE

In order to understand the proposed structure for the PR controller it is necessary to analyze the signals obtained from the SOGI resonant controller. The main idea of the double integrator is to generate a 180 phase shift to the input signal, which is achieved by means of two integrations, to obtain the resonance characteristic. If a closer look is made on Fig. 3, it is possible to get some general ideas.

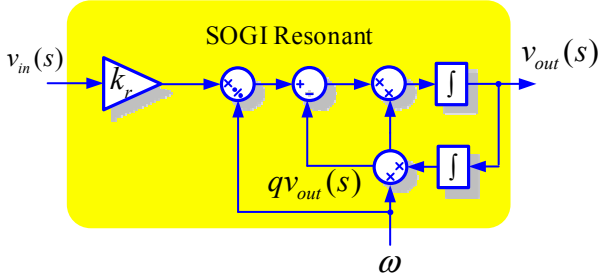


Fig. 3: Resonant of the input voltage – Characteristic points

Taking only the direct transfer function it would be just an integrator, which means that the value of $v_{in}(s)$ and $v_{out}(s)$ are 90 degree phase shifted due to the integration characteristic. If the second integration is made, the 180 phase shift is done and it is possible to be in phase with the input value, which means that $v_{in}(s)$ and $v_{out}(s)$ are in equal after the integrator get to the input nominal value.

The proposed structure is made by removing one of the integrators and adding the quadrature leg into the equations. If α input component is considered to be fixed to x -axis at the

initial time, the integral values are 90 degrees phase shifter. The integral values from both α and β are represented on Fig. 4.

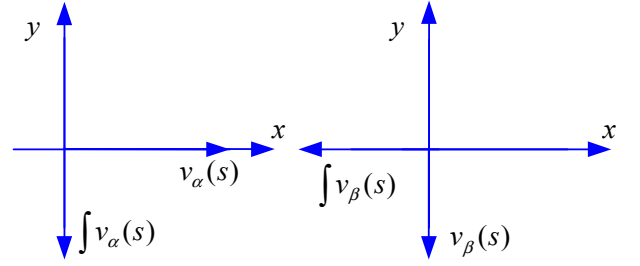


Fig. 4: Result on integration of α and β components

As it is possible to see in Fig. 4, $v_\alpha(s)$ and $\int v_\beta(s)$ are 180 degrees shifted, while $v_\beta(s)$ and $\int v_\alpha(s)$ are totally on phase. In order to have the same as the SOGI resonant, the proposed structure is presented on Fig. 5.

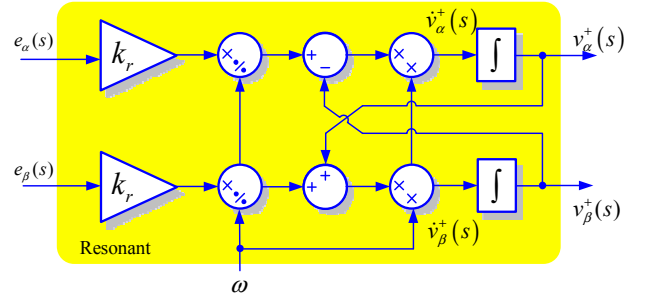


Fig. 5: Modified resonant controller structure

If the state space of this proposed schematic on the continuous domain is studied, the following transfer functions can be obtained.

$$e_\alpha = (i_\alpha^* - i_\alpha) \quad e_\beta = (i_\beta^* - i_\beta) \quad (7)$$

$$v_\alpha^+ = \frac{(e_\alpha \cdot k_r - v_\beta^+ \cdot \omega)}{s} \quad (8)$$

$$v_\beta^+ = \frac{(e_\beta \cdot k_r + v_\alpha^+ \cdot \omega)}{s} \quad (9)$$

By combining both equations (8) and (9) it is possible to create the resulting equations.

$$v_\alpha^+ = \frac{e_\alpha k_r s - e_\beta k_r \omega - v_\alpha^+ \omega^2}{s^2} \quad (10)$$

$$v_\beta^+ = \frac{e_\beta k_r s + e_\alpha k_r \omega - v_\beta^+ \omega^2}{s^2} \quad (11)$$

When those expressions are presented in a matrix relating the input and the output, the resulting matrix (12) matches perfectly the equations of the transformations of the PI on the dq -reference frame to the PR on the $\alpha\beta$ -reference frame.

$$\begin{bmatrix} v_{\alpha}^+ \\ v_{\beta}^+ \end{bmatrix} = \begin{bmatrix} \frac{k_r s}{s^2 + \omega^2} & \frac{k_r \cdot \omega}{s^2 + \omega^2} \\ \frac{-k_r \omega}{s^2 + \omega^2} & \frac{k_r s}{s^2 + \omega^2} \end{bmatrix} \begin{bmatrix} e_{\alpha} \\ e_{\beta} \end{bmatrix} \quad (12)$$

The addition of the proportional gain into the proposed resonant structure makes the final structure of the modified PR controller be the one presented on Fig. 6.

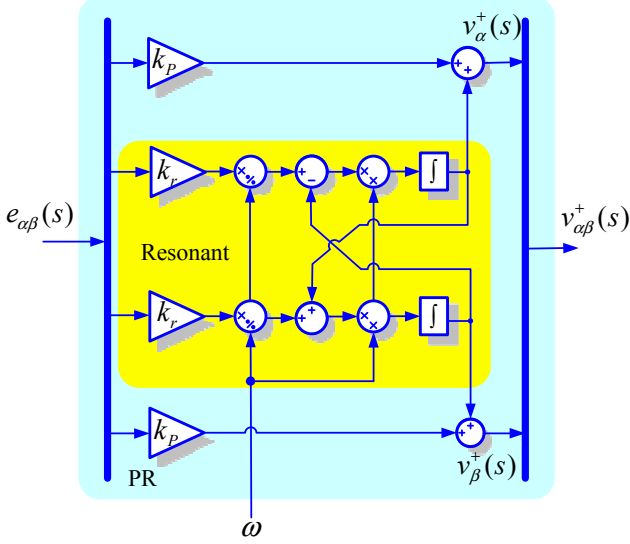


Fig. 6: Modified PR control structure on the continuous domain

IV. DECOUPLING TERMS

Studying the voltage at the inductor that acts as the interface between the inverter and the grid, it is possible to determine the next schematic on Fig. 7, representing the grid-connected inverter as a controlled voltage source.

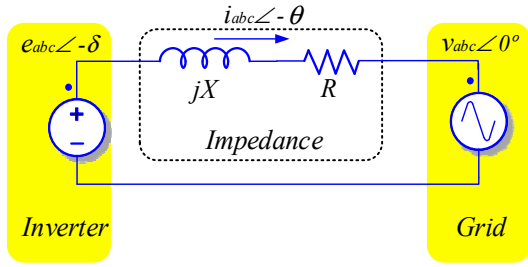


Fig. 7: Grid-connected inverter. Current going through the interconnection impedance.

Current through an impedance has been highly studied on the dq reference frame [6]. This study achieved that there is a coupling appearing on the dq frame from each component. The dynamic state coupling can be represented on dq frame as:

$$\Delta v_{Ld}(t) = v_d(t) - e_d(t) - Ri_d(t) + i_q(t) \omega L \quad (13)$$

$$\Delta v_{Lq}(t) = v_q(t) - e_q(t) - Ri_q(t) - i_d(t) \omega L \quad (14)$$

On the $\alpha\beta$ -reference frame happens something similar when the voltage deviation at the inductor is exposed. The corresponding equation appears as:

$$\frac{di_{\alpha}(t)}{dt} L = v_{\alpha}(t) - e_{\alpha}(t) - Ri_{\alpha}(t) \quad (15)$$

$$\frac{di_{\beta}(t)}{dt} L = v_{\beta}(t) - e_{\beta}(t) - Ri_{\beta}(t) \quad (16)$$

Assuming that the frequency of the grid is 50 Hz, and the components are mostly pure sinusoidal, it is possible by derivation of equations (15) and (16) on time and some reorganization of the parameters to obtain the final expression of the voltage deviation during transients as:

$$\Delta v_{L_{\alpha}}(t) = v_{\alpha}(t) - e_{\alpha}(t) - Ri_{\alpha}(t) + i_{\beta}(t) \omega L \quad (17)$$

$$\Delta v_{L_{\beta}}(t) = v_{\beta}(t) - e_{\beta}(t) - Ri_{\beta}(t) - i_{\alpha}(t) \omega L \quad (18)$$

The resulting equation (17) and (18) expresses that there exists a coupling between the components on the $\alpha\beta$ -reference frame, and it matches perfectly to the theory of the dq -reference frame, having both the exact same value when performing the decoupling matrix. Finally if the decoupling terms on the $\alpha\beta$ frame are joined with the modified PR controller, the structure becomes the one on Fig. 8.

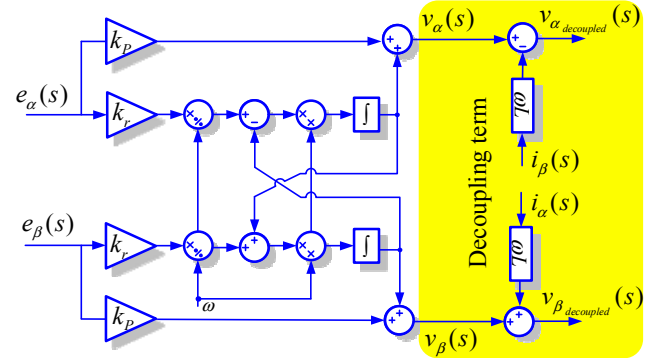


Fig. 8: Decoupling matrix added to the PR modified structure

In order to validate the equations, the modified PR controller, the SOGI classical PR controller and the PI controller are going to be compared through simulation. Also the decoupling matrix either on the dq and the $\alpha\beta$ reference frame are going to be compared.

V. SIMULATION RESULTS

On this section, a comparison between the PI controller and the different PR controllers is going to be done. The simulation setup will be composed by two grid-tied inverter with the parameters showed on Table. 1. Those two power converter have different controllers in order to test its dynamics. The decoupling terms are going to be enabled and disable on the simulations in order to see their effect on steady and dynamic state.

The current controller will be controlling the grid side current, in order to amplify the delay on the current due to the inductor. This delay will add to the controller more difficulties to control the current; therefore the decoupling action and the difference on the controller will be better reflected on the simulation.

Inverter 100kVA – Elements	
Fs	3150 Hz
Ts	6300 Hz
L1	777 μ H
Rc	0.5 Ω
C	66 μ F
L2	294 μ H
Lg	1000 μ H

Table. 1: Inverter 100kVA – Elements on the system

A. PI Controller vs SOGI Classic PR Controller

The parameters of both controllers are presented on Table. 2. PR and PI controllers have the same control parameters, those parameters are forced to be the same in order to see the difference of the each controller in steady and dynamic state response.

PR and PI current controller parameters	
$k_{pr} = k_{pi}$	0.5
$k_r = k_i$	100

Table. 2: Parameters of the SOGI PR controller and the PI controller

On this first test the comparison between the SOGI classical PR controller and the PI controller is made. In $t = 0.2s$ a power step to 40kW is generated on each power converter. The red signal represents the response of the PR controller, which is producing an oscillation of approximately 100Hz, mainly due to the negative sequence control on a relatively weak grid. As it is shown on Fig. 9 the response of the SOGI PR controller and the PI controller is compared. The result obtained from this simulation is that there is no error at the steady state, however there is a strong difference on the dynamic state, affecting the overall stability of the system during transients.

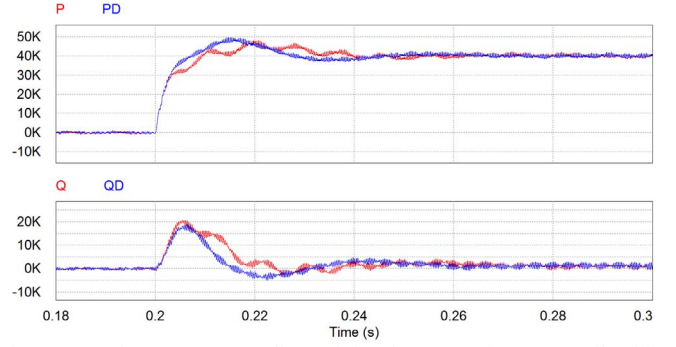


Fig. 9: General SOGI PR Controller (red signal) compared to PI controller (blue signal)

Once the decoupling term is added to the simulation above, the result obtained is reflected on Fig. 10. The steady state error remains zero and the dynamic transient of the PR controller is improved from the previous action, which did not have the decoupling matrix. That means that the decoupling matrix on the dq and the $\alpha\beta$ frame improves the dynamic state of the controller.

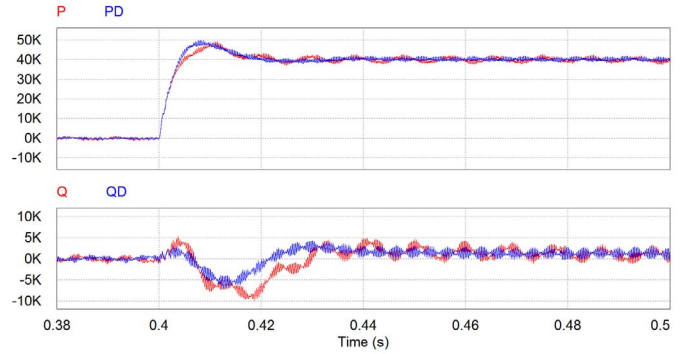


Fig. 10: SOGI PR Controller decoupling (red signal) compared to PI decoupled (blue signal)

B. PI Controller vs Modified PR Controller

The parameters of both controllers are presented on Table. 3. On this case the parameters remain equal for both controllers in order to compare the results with the SOGI classical PR controller.

PR and PI current controller parameters	
$k_{pr} = k_{pi}$	0.5
$k_r = k_i$	100

Table. 3: Parameters of the modified PR controller and the PI controller

The modified PR Controller is going to be compared to the PI controller. The same power step is going to be tested, in order to compare this simulation to the results of the previous one. In $t = 0.2$ a power step to 40 kW is generated on each power converter. Once the step is generated, there is no oscillation of 100Hz during the transient step. The steady state error remains zero in both controllers, and the dynamic performance of the PR controller is improved from the SOGI PR controller as it is presented on Fig. 11.

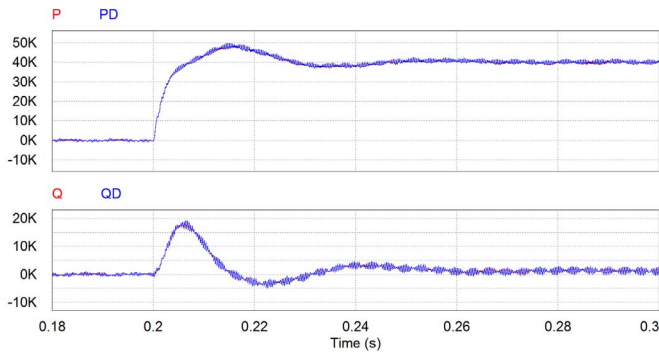


Fig. 11: Modified PR Controller structure (red signal) compared to PI controller (blue signal)

The decoupling terms are implemented on the simulation only on the PI controller in order to see the difference on dynamic response of both controllers. Fig. 12 presents the benefit from including the decoupling terms into the simulation. Not only the coupling between active and reactive power is reduced, but the overall speed of the power step is increased.

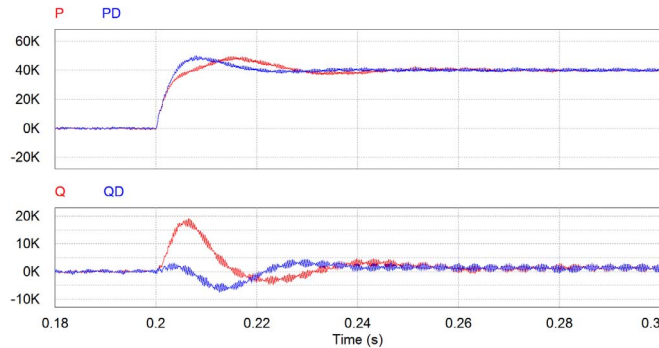


Fig. 12: Modified PR Controller structure (red signal) compared to PI controller with the decoupling matrix (blue signal)

Finally, when the decoupling terms are included in both of the controllers, the results in the one presented on Fig. 13. The dynamic response of both controllers is equivalent on two different reference frame.

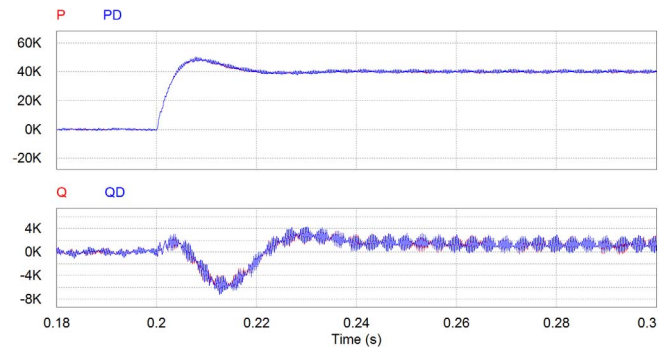


Fig. 13: Modified PR Controller decoupling terms (red signal) compared to PI decoupling terms (blue signal)

VI. CONCLUSION

A modified PR structure adapting the performance of the traditional PR controller, and making it match perfectly the dynamic of the PI is achieved. A proposed decoupling on the

$\alpha\beta$ is also discussed and finally appears to have the same dynamics and effects than the dq -reference frame decoupling.

The effectiveness of the modified PR controller and the decoupling matrix on the $\alpha\beta$ -reference frame has been verified by simulations, where the results show that the modified PR controller and the PI controller provide the same performance under power steps. Meaning that the dq -reference frame and the $\alpha\beta$ -reference frame have no difference neither in current controller performance or the decoupling terms as they are perfectly equal in steady and dynamic state.

REFERENCES

- [1] E. Challenge, "ENTSO-E RECOMMENDATIONS TO HELP ACHIEVE EUROPE 'S ENERGY AND CLIMATE EUROPE ' S ENERGY CHALLENGE," 2014.
- [2] Y. Yang, P. Enjeti, F. Blaabjerg, and H. Wang, "Wide-Scale Adoption of Photovoltaic Energy: Grid Code Modifications Are Explored in the Distribution Grid," *Industry Applications Magazine, IEEE*, vol. 21, no. 5, pp. 21–31, 2015.
- [3] A. Marinopoulos, F. Papandrea, M. Reza, S. Norrga, F. Spertino, and R. Napoli, "Grid integration aspects of large solar PV installations: LVRT capability and reactive power/voltage support requirements," *PowerTech, 2011 IEEE Trondheim*, pp. 1–8, 2011.
- [4] "ENTSO-E Network Code for Requirements for Grid Connection Applicable to all Generators 2015," *Eff. Br. mindfulness Interv. acute pain Exp. An Exam. Individ. Differ.*, vol. 1, 2015.
- [5] J. Rocabert, A. Luna, F. Blaabjerg, and P. Rodríguez, "Control of Power Converters in AC Microgrids," *IEEE Trans. Power Electron.*, vol. 27, no. 11, pp. 4734–4749, 2012.
- [6] M. Reyes, P. Rodríguez, S. Vazquez, A. Luna, R. Teodorescu, and J. M. Carrasco, "Enhanced Decoupled Double Synchronous Reference Frame Current Controller for Unbalanced Grid-Voltage Conditions," *IEEE Trans. Power Electron.*, vol. 27, no. 9, pp. 3934–3943, 2012.
- [7] D. N. Zmood, D. G. Holmes, and G. Bode, "Frequency domain analysis of three phase linear current regulators," *Industry Applications Conference, 1999. Thirty-Fourth IAS Annual Meeting. Conference Record of the 1999 IEEE*, vol. 2, pp. 818–825 vol.2, 1999.
- [8] D. N. Zmood, D. G. Holmes, and G. H. Bode, "Frequency-domain analysis of three-phase linear current regulators," *Industry Applications, IEEE Transactions on*, vol. 37, no. 2, pp. 601–610, 2001.
- [9] S. Buso and P. Mattavelli, *Digital Control in Power Electronics, 2nd Edition*. Morgan & Claypool, 2015.
- [10] P. Rodríguez, A. Luna, I. Candela, R. Teodorescu, and F. Blaabjerg, "Grid synchronization of power converters using multiple second order generalized integrators," in *2008 34th Annual Conference of IEEE Industrial Electronics*, 2008, pp. 755–760.
- [11] W. Zhang, C. Citro, A. M. Cantarellas, D. Remon, A. Luna, and P. Rodríguez, "Tuning of proportional resonant controllers for three phase PV power converters with LCL+trap filter," *2014 IEEE PES T&D Conference and Exposition*. pp. 1–5, 2014.
- [12] D. N. Zmood and D. G. Holmes, "Stationary frame current regulation of PWM inverters with zero steady-state error," *IEEE Trans. Power Electron.*, vol. 18, no. 3, pp. 814–822, 2003.
- [13] R. Teodorescu, F. Blaabjerg, M. Liserre, and P. C. Loh, "Proportional-resonant controllers and filters for grid-connected voltage-source converters," *IEE Proc. - Electr. Power Appl.*, vol. 153, no. 5, pp. 750–762, 2006.
- [14] P. Rodríguez, A. Luna, I. Candela, R. Mujal, R. Teodorescu, and F. Blaabjerg, "Multiresonant Frequency-Locked Loop for Grid Synchronization of Power Converters Under Distorted Grid Conditions," *IEEE Transactions on Industrial Electronics*, vol. 58, no. 1, pp. 127–138, 2011.